ЖУРНАЛ СТРУКТУРНОЙ ХИМИИ

2013. Том 54, № 1 *Январь – февраль* *С. 40 – 47*

UDC 541.6:543.422

THEORETICAL STUDY ON THE STRUCTURES AND PROPERTIES OF $(Br_2AlN_3)_n$ (n = 1—4) CLUSTERS

Q.Y. Xia, D.X. Ma, D.J. Li, W.W. Zhao

School of Chemistry and Chemical Engineering, *Linyi University, Linyi 276005, P. R. China*
E-mail: xiaqiying@163.com

Received September, 12, 2011

To look for the single-source precursors, the structures and properties of $(Br_2AlN_3)_n$ (n = 1—4) clusters are studied at the B3LYP/6-311+G* level. The optimized $(Br_2AlN_3)_n$ (n = 2—4) clusters all possess cyclic structures containing Al—N_α—Al linkages. The relationships between the geometrical parameters and the oligomerization degree n are discussed. The gas-phase structures of the trimers prefer to exist in the *boat*-twisting conformation. As for the tetramer, the most stable isomers have the S_4 symmetry structure. The IR spectra are obtained and assigned by the vibrational analysis. The thermodynamic properties are linearly related with the oligomerization degree n as well as with the temperature. Meanwhile, the thermodynamic analysis of the gas-phase reaction suggests that the oligomerization be exothermic and favorable under high temperature.

K e y w o r d s: $(Br_2AlN_3)_n$ (n = 1—4) clusters, density functional theory (DFT), structural feature, IR spectra, thermodynamic properties.

INTRODUCTION

Aluminum nitrides (AlN) have attracted increasing interest for microelectronics and optoelectronics due to their excellent material properties such as a wide band gap, low electrical and high thermal conductivity, high melting temperature, hardness, and good chemical stability [1—3]. The most successful approach to AlN involves the reaction of trimethylaluminum ($AlMe_3$) with ammonia (NH_3) at a temperature in excess of 1050 °C [4]. However, such elevated growth temperatures may lead to unintentional nitrogen vacancies limiting the *p*-doping capability. Alternative synthetic routes to stoichiometric AlN materials involve the use of single-source precursors containing strong Al—N bonds in the hope of lowering the reaction temperature [5]. Other possible advantages include the elimination of the inefficient use of ammonia, the minimization of parasitic pre-reactions in the gas phase, and the simplification of the processes.

Because the azide group seems to be the optimal build-in nitrogen source and nitrides were successfully deposited without additional nitrogen sources, particularly promising are single-source precursors that contain the azide (N_3) ligand as the nitrogen source [6—18]. The product formed has a high degree of carbon contamination due to pyrolysis of the organic substituent. So, McMurran *et al.* reported several related routes for the GaN synthesis utilizing a new class of inorganic azide compounds that incorporate hydrogen and halide ligands [14—18] instead of organic groups. However, the inorganic metal azide clusters of aluminum have seemingly been the subject of little experimental studies [19].

The reasons are the difficulties arising in the experimental detection. Reliable structures, IR spectra, and thermodynamic properties of many gas-phase precursors are not at all well-documented, and theoretical predictions for the single-source precursors that contain the azide (N_3) ligand thus become

an important ongoing task. Meanwhile, motivated by and based on previously studies on the clusters such as $(H_2AlN_3)_n$ (n = 1—4) [20], $(MYR_2)_n$ (M = B, Al, Ga; Y = N, P, As; R = H, CH_3; n = 1, 2) [21], and $(MYH_2)_4$ (M = B, Al, Ga; Y = N, P, As) [22], we performed density functional theory (DFT) investigations on the structural features, energies, and IR spectra of $(Br_2AlN_3)_n$ (n = 1—4) clusters and also as the contributions of the temperature and the oligomerization degree n to the thermodynamic properties were established. We hope the calculated vibrational spectra can provide references for experimentalists. The thermodynamic properties of $(Br_2AlN_3)_n$ (n = 1—4) clusters are expected to provide useful information for the molecular design of novel aluminum azides. In addition, the results shed some light on the emergence of their bulk-like behavior with an increase in the cluster size.

COMPUTATIONAL METHODS

The calculations performed in this study were made using the Gaussian03 program package with the default convergence criteria [23]. All the clusters in Fig. 1 generated from the ChemBats3D software were fully optimized by the Berny method at the DFT-B3LYP/6-311+G* level [24, 25]. The harmonic vibrational analyses were performed subsequently on each optimized structure at the same level in order to characterize the nature of the stationary points and determine the zero-point vibrational energy corrections. Since the DFT calculated harmonic vibrational frequencies are usually larger than those observed experimentally, they are scaled using a factor of 0.96 to correct the systematic errors [26]. Based on the principle of statistical thermodynamics [27], the thermodynamics standard molar heat capacity ($C^0_{p,m}$), standard molar entropy (S^0_m), and standard molar enthalpy (H^0_m) of $(Br_2AlN_3)_n$ (n = 1—4) from 200 K to 800 K are obtained using a self-compiled program.

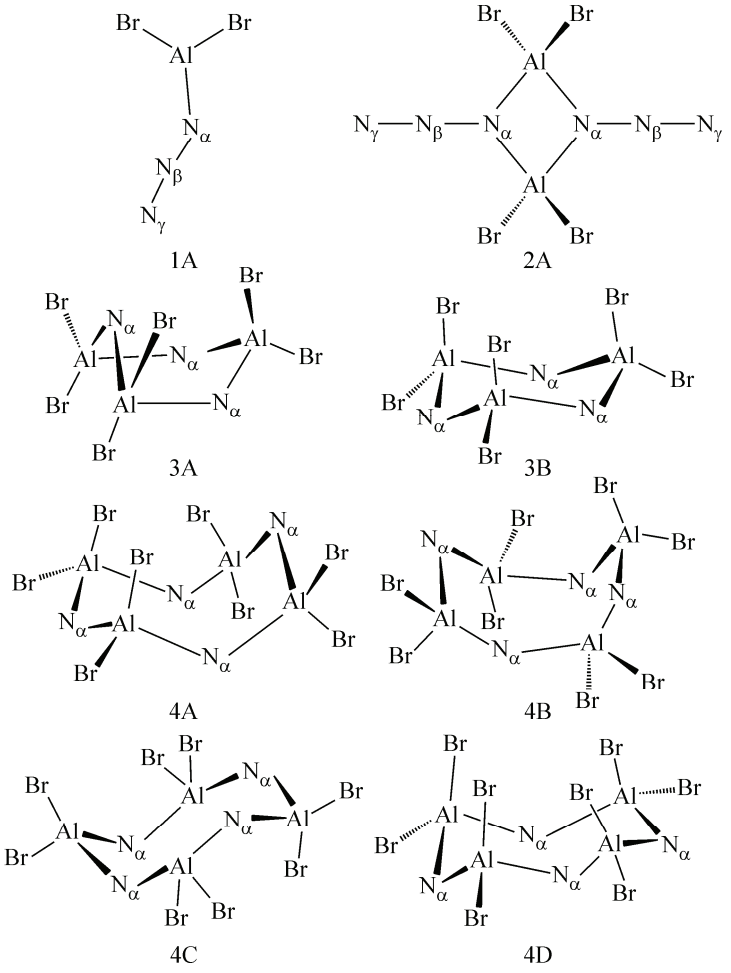

Fig. 1. Optimized geometries of $(Br_2AlN_3)_n$ (n = 1—4) clusters (N_β and N_γ atoms in trimers and tetramers are omitted for clarity)

RESULTS AND DISCUSSIONS

Geometries and energies. All the optimized structures were characterized to be the true local energy minima on the potential energy surface without any imaginary frequency. Monomer species (Br_2AlN_3) is studied only as starting points for the oligomerization. As shown in Fig. 1, Br_2AlN_3 is a planar molecule with C_s symmetry (connectivity: $Br_2Al—N_\alpha—N_\beta—N_\gamma$ Fig. 1, 1A). The dimer $(Br_2AlN_3)_2$ with D_{2h} symmetry is produced by two Br_2AlN_3 oligomerizing via the α-N atoms, containing the $Al—N_\alpha—Al$ linkages. The dimer $(Br_2AlN_3)_2$ is still unknown, however, the dimeric structure has been observed for the group IIIA metallic azide clusters, such as $[(CH_3)_2MN_3)]_2$ (M = Al, Ga) [28, 29], $(H_2AlN_3)_2$ [20], and $(H_2GaN_3)_2$ [14, 15, 30]. We have examined two new types of a trimer $(Br_2AlN_3)_3$, as shown in Fig. 1: a *boat*-twisting conformation 3A (symmetric C_1) and a *chair*—like conformation 3B (symmetric C_s). Al atoms are also connected by the N_α atoms of azide groups to form a six-membered ring, which is similar to the structures of other previously determined group IIIA azides, such as $(H_2AlN_3)_3$ [20], $(R_2AlN_3)_3$ (R = Me, Et) [12, 13, 28, 29], $(H_2GaN_3)_3$ [14, 15, 30], $(Cl_2GaN_3)_3$ [18], and $[(CH_3)BrGaN_3]_3$ [31]. The geometries of $(Br_2AlN_3)_4$ predicted at the B3LYP/6-311+G* level are presented in Fig. 1. Structures 4A—4D reveal the presence of an eight—membered ring structure incorporating bridging azide with $Al—N_\alpha—Al$ linkages. They belong to C_s (4A), S_4 (4B), C_i (4C) and C_2 (4D) symmetry respectively, of which only the S_4 symmetry structure with N_3 alternatively up and down has been suggested for the tetramers $[(CH_3)ClAlN_3]_4$ and $[(CH_3)BrAlN_3]_4$ [8] of aluminum azides, and the other three structures have not been found except that our group have reported [20]. As shown by the optimized structures of $(Br_2AlN_3)_n$ (n = 2—4) clusters in Fig. 1, the $Al—N_\alpha$ bonds form easily, and Al—Al and $N_\alpha—N_\alpha$ bonds are not found in the clusters.

The ranges of the optimized bond lengths and angles were presented in Table 1. In the $(Br_2AlN_3)_n$ (n = 1—4) clusters, the bond lengths of 1.214—1.256 Å for $N_\alpha—N_\beta$ bonds and 1.118—1.133 Å for

Table 1

Ranges of bond lengths (Å), *bond angles* (deg.), *and energies* ($kJ \cdot mol^{-1}$) *for the titled clusters optimized at the* B3LYP/6-311+G* *level*

Parametr	1A	2A	3A	3B
$N_\beta—N_\gamma$	1.133	1.123	1.118—1.121	1.121
$N_\alpha—N_\beta$	1.214	1.235	1.249—1.255	1.251
$Al—N_\alpha$	1.777	1.952	1.958—1.965	1.967—1.968
Al—Br	2.238—2.247	2.264	2.266—2.275	2.257—2.279
$N_\alpha—N_\beta—N_\gamma$	176.0	180.0	179.5—179.7	179.7—179.9
$N_\beta—N_\alpha—Al$	140.7	130.0	116.0—119.1	116.0—116.2
$Al—N_\alpha—Al$		100.1	123.6—128.0	127.7—128.0
$N_\alpha—Al—N_\alpha$		79.9	96.8—99.5	99.7—100.0
E	–14585093.4	–29170382.4	–43755586.2	–43755568.5
ZPE	41.7	89.3	134.8	134.3
Parametr	4A	4B	4C	4D
$N_\beta—N_\gamma$	1.119—1.120	1.119	1.120—1.121	1.120—1.121
$N_\alpha—N_\beta$	1.254—1.256	1.255	1.253—1.254	1.254—1.255
$Al—N_\alpha$	1.968—1.983	1.951—1.972	1.964—1.972	1.974—1.986
Al—Br	2.255—2.279	2.268—2.278	2.263—2.275	2.246—2.286
$N_\alpha—N_\beta—N_\gamma$	179.6—179.9	179.4	179.5—179.7	179.0—179.7
$N_\beta—N_\alpha—Al$	113.8—116.2	114.8—117.2	114.0—117.0	110.9—115.5
$Al—N_\alpha—Al$	128.5—129.5	127.3	127.6—130.2	129.8—134.3
$N_\alpha—Al—N_\alpha$	100.6—102.1	102.5	101.9—102.6	98.8—102.4
E	–58340751.7	–58340782.1	–58340768.0	–58340734.9
ZPE	179.5	180.5	179.9	178.8

N_β—N_γ bonds are very close to the N=N double bond length (1.250 Å) and N≡N triple bond length (1.100 Å) respectively. Obviously, there are two distinct N—N distances in the azide group, with the shorter one corresponding to the terminal N—N bonds. For the Br_2AlN_3 monomer, the bond angle of N_α—N_β—N_γ is 176.0°, indicating that the azide group is slightly bent. As for $(Br_2AlN_3)_n$ (n = 2—4), azide groups are nearly linear with the N_α—N_β—N_γ bond angles of 179.0—180.0°. There are some changes in the geometric parameters with increasing n value; e.g., the N_α—N_β bond lengths are gradually elongated from 1.214 Å up to about 1.256 Å. The same trends in bond lengths are observed for Al—Br (from 2.238 Å to 2.286 Å) and Al—N_α bonds (from 1.777 Å to 1.986 Å). On the contrary, the N_β—N_γ bond lengths gradually become shorter from 1.133 Å to around 1.120 Å with increasing n. Outside of the rings, the increasing N_α—N_β and Al—Br bond lengths, as compared to the monomer, show that it could easily eliminate N_2 (N_β—N_γ) and Br^- groups to yield AlN material. The N_β—N_α—Al bond angles decrease distinctly from 140.7° to 110.9° as the clusters enlarge, while the N_α—Al—N_α and Al—N_α—Al bond angles increase distinctly from 79.9° to 102.6° and from 100.1° to 134.3° respectively. As seen from Table 1, the obtained Al—N_α—Al bond angles are consistently larger than the N_α—Al—N_α bond angles in the cyclic clusters. Obviously, the trends of average geometrical parameters are similar to those reported previously for $(H_2AlN_3)_n$ (n = 1—4) [20] and $[(CH_3)_2AlN_3]_n$, (n = 1—3) clusters [28, 29] with increasing oligomerization degree n.

In order to obtain an estimation of the thermodynamic stability of Br_2AlN_3 with respect to its oligomerization to $(Br_2AlN_3)_{2—4}$, the values of the total energy and zero point energy (*ZPE*) for all the clusters are calculated at the B3LYP/6-311+G* level and listed in Table 1. The energies show that the order of stability is as follows: 3A > 3B and 4B > 4C > 4A > 4D. The more attractive trimer 3A possessing the *boat*-twisting conformation is about 17.77 kJ·mol^{-1} lower in energy than the trimer 3B possessing the *chair*—like conformation. As for the tetramer, the energy difference is about 14.16 ~ 47.19 kJ·mol^{-1}.

IR spectrum. As is well known, IR spectra reflect not only the basic properties of compounds, but also the effective measures to analyze or identify substances. Besides, they have a direct relationship with the thermodynamic properties. Heretofore only little experimental data on the IR spectra has been reported for the titled compounds [19], and no systematic studies on the $(Br_2AlN_3)_n$ (n = 1—4) clusters have been performed. Therefore, the theoretical predictions of their IR spectra are of great importance for both theoretical and practical reasons. The fundamental vibrational frequencies were obtained from the B3LYP/6-311+G* calculations using analytical second-order derivatives at the optimized geometries, and the simulated IR spectra for the titled compounds based on the scaled harmonic vibrational frequencies are presented in Fig. 2, where the intensity is plotted against the frequency. It is difficult to assign all bands due to the complexity of vibrational modes, so here only some typical vibrational modes are assigned and discussed, which would facilitate the assignment of the observed peaks. Fig. 2 shows that there are three main characteristic regions for the $(Br_2AlN_3)_n$ (n = 1—4) clusters, which are associated with N_3 asymmetric and symmetric stretching, and the fingerprint region in the lower frequencies.

The IR vibrational peaks of all clusters with the strongest absorption intensities locate in the region 2192—2228 cm^{-1}, corresponding to N_3 asymmetric stretching vibrations, and in this region, the number of vibrations equals that of azide groups. For example, 1A has one band at 2228 cm^{-1} and 2A has two bands at 2219 cm^{-1} and 2227 cm^{-1}. Another remarkable signal peak in the region 1174—1394 cm^{-1} is associated with N_3 symmetric stretching vibrations. In agreement with N_3 asymmetric stretching vibrations, in this region, the number of vibrations also equals that of azido groups. For example, 4B has four bands at 1194 cm^{-1}, 1197 cm^{-1}, 1197 cm^{-1}, and 1205 cm^{-1}. The region less than 733 cm^{-1} is the fingerprint region, which can be used to identify and distinguish the isomeric configurations. The relatively weak peaks in this region are mainly caused by the stretching of rings, the asymmetric, symmetric stretching and wagging of $AlBr_2$, and the N_3 deformation vibrations, etc.

Moreover, the oligomerization degree n has an effect on the vibrational frequencies and intensities for the most stable cluster (1A, 2A, 3A, 4B). The N_3 asymmetric stretching moves to higher frequencies (hypsochromic phenomenon) as the cluster becomes larger, however, the N_3 symmetric stretching moves to lower frequencies (bathochromic phenomenon).

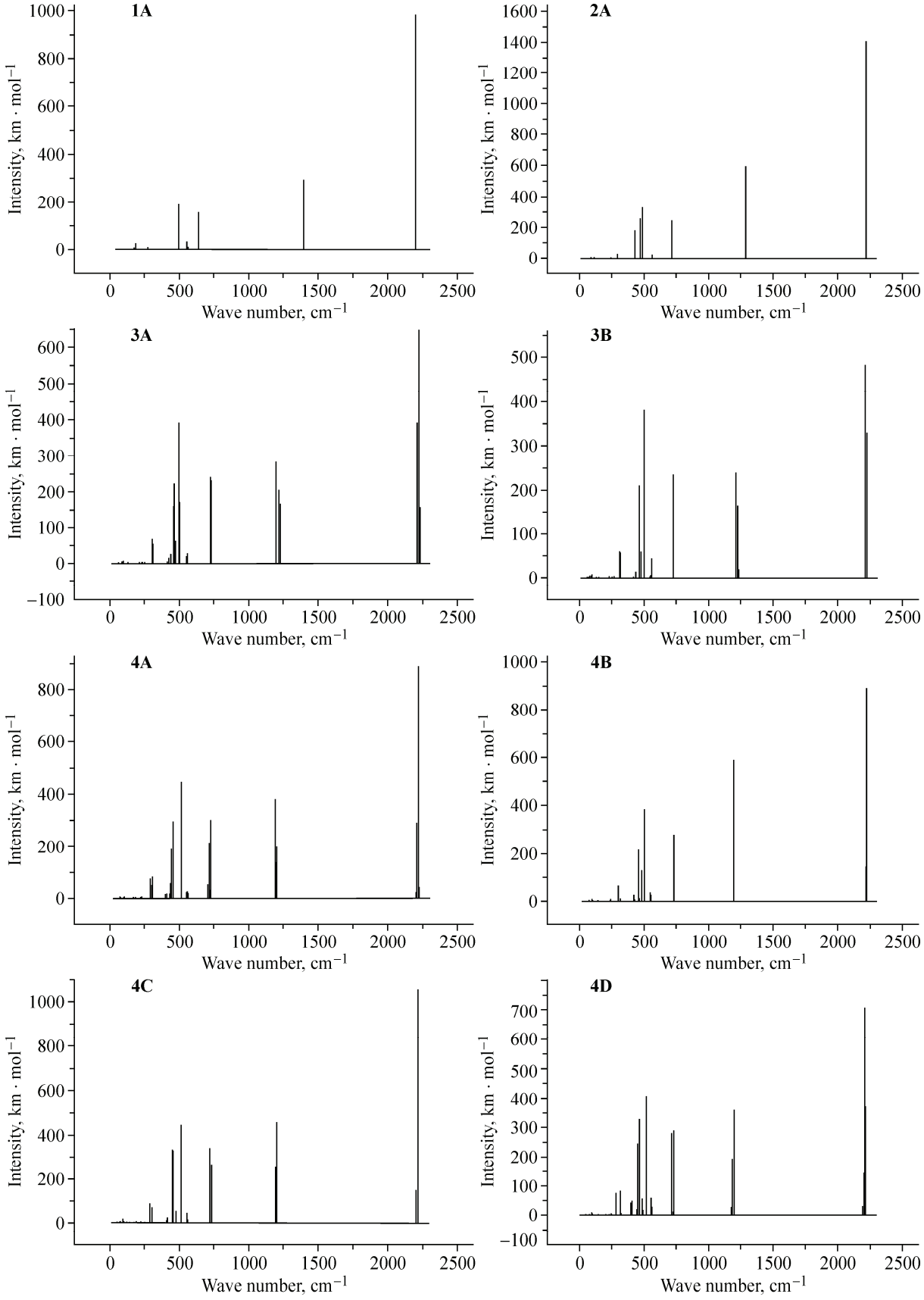

Fig. 2. IR spectra of $(Br_2AlN_3)_n$ (n = 1—4) clusters simulated at the B3LYP/6-311+G* level

Table 2

Thermodynamic properties of $(Br_2AlN_3)_n$ (n = 1—4) *clusters at different temperatures* [a]

	T	200	298.2	300	400	500	600	700	800
1A	$C^0_{p,m}$	88.27	99.92	100.08	107.3	112.23	115.89	118.73	120.99
	S^0_m	300.68	338.29	338.91	368.76	393.26	414.06	432.14	448.15
	H^0_m	13.17	22.45	22.64	33.03	44.02	55.44	67.17	79.16
2A	$C^0_{p,m}$	183.49	211.67	212.06	228.78	239.76	247.65	253.63	258.3
	S^0_m	464.12	543.17	544.48	607.96	660.26	704.71	743.35	777.53
	H^0_m	25.42	44.95	45.34	67.45	90.91	115.3	140.38	165.98
3A	$C^0_{p,m}$	273.92	317.09	317.7	343.44	360.23	372.18	381.15	388.11
	S^0_m	641.13	759.35	761.31	856.52	935.08	1001.87	1059.94	1111.31
	H^0_m	36.44	65.64	66.22	99.38	134.62	171.27	208.96	247.43
3B	$C^0_{p,m}$	282.67	325.79	326.39	352.05	368.78	380.68	389.62	396.55
	S^0_m	681.21	802.92	804.94	902.64	983.11	1051.45	1110.83	1163.33
	H^0_m	38.22	68.28	68.89	102.91	139	176.51	215.04	254.36
4A	$C^0_{p,m}$	374.29	431.99	432.8	467.09	489.41	505.24	517.12	526.31
	S^0_m	788.07	949.36	952.03	1081.62	1188.41	1279.11	1357.92	1427.6
	H^0_m	49.37	89.2	90	135.13	183.03	232.8	283.95	336.14
4B	$C^0_{p,m}$	381.7	439.59	440.4	474.84	497.25	513.15	525.08	534.31
	S^0_m	807.76	972.04	974.77	1106.57	1215.09	1307.23	1387.26	1458.01
	H^0_m	50.78	91.36	92.17	138.07	186.75	237.31	289.24	342.23
4C	$C^0_{p,m}$	382.1	439.81	440.62	474.99	497.39	513.3	525.22	534.46
	S^0_m	819.96	984.36	987.08	1118.94	1227.49	1319.65	1399.71	1470.47
	H^0_m	51.05	91.65	92.46	138.38	187.07	237.64	289.6	342.6
4D	$C^0_{p,m}$	382.7	440.34	441.15	475.48	497.83	513.69	525.57	534.76
	S^0_m	844.94	1009.56	1012.29	1144.29	1252.95	1345.19	1425.3	1496.11
	H^0_m	51.4	92.05	92.87	138.84	187.57	238.19	290.18	343.22

[a] Units: T (K), $C^0_{p,m}$ ($J \cdot mol^{-1} \cdot K^{-1}$), S^0_m ($J \cdot mol^{-1} \cdot K^{-1}$), H^0_m ($kJ \cdot mol^{-1}$).

Thermodynamic properties. The thermodynamic functions, such as the standard molar heat capacity ($C^0_{p,m}$), the standard molar entropy (S^0_m), and the standard molar enthalpy (H^0_m) are also important parameters for the compounds and are necessary for predicting the reactive properties of chemical reactions. However, hitherto we are not aware of any experimental results for the thermodynamic properties of the titled compounds. In this section, the thermodynamic functions ($C^0_{p,m}$, S^0_m, and H^0_m) ranging from 200 K to 800 K are evaluated and presented in Table 2. Firstly, as can be seen, with an increase in the temperature the calculated entropies of $(Br_2AlN_3)_n$ (n = 1 to 4) clusters increase evidently. This is because the main contributions to the entropy are from the translations and rotations of the molecules at lower temperatures, whereas the vibrational motion is intensified at higher temperatures and makes more contributions to the entropy. The same is true of the enthalpy and heat capacity. For intuitive illustration, 1A (monomer) was taken from the titled clusters as typical examples to show

the quantitative relationships between the thermodynamic functions and the temperature. The corresponding equations can be expressed as follows:

$$C^0_{p,m} = 65.8229 + 0.1366T - 8.5854 \times 10^{-5}T^2,$$

$$S^0_m = 221.1785 + 0.4507T - 2.1100 \times 10^{-4}T^2,$$

$$H^0_m = -5.3561 + 0.0866T + 2.3986 \times 10^{-5}T^2,$$

and the correlation coefficients R^2 are 0.9924, 0.9991, and 1.0000 respectively.

It is obvious that as the temperature increases, the increments of $C^0_{p,m}$ and S^0_m both decrease, but that of H^0_m increases constantly. However, since the coefficients of T^2 are very small, these correlations approximate linear equations. In other words, the thermodynamic functions of $(Br_2AlN_3)_n$ (n = 1 to 4) clusters increase linearly with the temperature.

Secondly, with increasing oligomerization degree n the thermodynamic functions of the most stable clusters all increase monotonically, and these correlations can be described directly by the following equations at 298.2 K:

$$C^0_{p,m} = -14.040 + 112.443n,$$

$$S^0_m = 123.855 + 211.743n,$$

$$H^0_m = -0.755 + 22.742n.$$

The correlation coefficients are all more than 0.99, and $C^0_{p,m}$, S^0_m, and H^0_m increase respectively by the average values of 112.4 $J \cdot mol^{-1} \cdot K^{-1}$, 211.7 $J \cdot mol^{-1} \cdot K^{-1}$, and 22.7 $kJ \cdot mol^{-1}$ with each additional

Table 3

Oligomerization entropies, enthalpies and gibbs free energies at different temperatures [a]

Processes	T	200	298.2	300	400	500	600	700	800
1A → (1/2)2A	ΔS	–68.62	–66.71	–66.67	–64.78	–63.13	–61.71	–60.47	–59.39
	ΔH	–95.35	–94.87	–94.86	–94.20	–93.46	–92.68	–91.87	–91.06
	ΔG	–81.63	–74.98	–74.86	–68.29	–61.89	–55.66	–49.55	–43.56
1A → (1/3)3A	ΔS	–86.97	–85.17	–85.14	–83.25	–81.57	–80.10	–78.83	–77.71
	ΔH	–99.90	–99.44	–99.44	–98.78	–98.02	–97.22	–96.39	–95.56
	ΔG	–82.50	–74.05	–73.90	–65.48	–57.24	–49.16	–41.21	–33.39
1A → (1/3)3B	ΔS	–73.61	–70.65	–70.60	–67.88	–65.56	–63.58	–61.86	–60.37
	ΔH	–93.52	–92.78	–92.77	–91.82	–90.78	–89.70	–88.58	–87.47
	ΔG	–78.80	–71.72	–71.59	–64.67	–58.00	–51.55	–45.28	–39.17
1A → (1/4)4A	ΔS	–103.66	–100.95	–100.90	–98.36	–96.16	–94.28	–92.66	–91.25
	ΔH	–92.28	–91.60	–91.59	–90.70	–89.71	–88.69	–87.63	–86.57
	ΔG	–71.54	–61.50	–61.32	–51.36	–41.63	–32.12	–22.77	–13.57
1A → (1/4)4B	ΔS	–98.74	–95.28	–95.22	–92.12	–89.49	–87.25	–85.33	–83.65
	ΔH	–99.28	–98.41	–98.40	–97.32	–96.14	–94.92	–93.66	–92.41
	ΔG	–79.53	–70.00	–69.83	–60.47	–51.39	–42.56	–33.94	–25.49
1A → (1/4)4C	ΔS	–95.69	–92.20	–92.14	–89.03	–86.39	–84.15	–82.21	–80.53
	ΔH	–95.83	–94.96	–94.95	–93.86	–92.67	–91.45	–90.19	–88.93
	ΔG	–76.69	–67.46	–67.30	–58.25	–49.48	–40.96	–32.64	–24.50
1A → (1/4)4D	ΔS	–89.45	–85.90	–85.84	–82.69	–80.02	–77.76	–75.82	–74.12
	ΔH	–87.73	–86.85	–86.83	–85.73	–84.54	–83.30	–82.03	–80.76
	ΔG	–69.84	–61.23	–61.08	–52.65	–44.53	–36.64	–28.96	–21.47

[a] Units: T (K), ΔS ($J \cdot mol^{-1} \cdot K^{-1}$), ΔH ($kJ \cdot mol^{-1}$), ΔG ($kJ \cdot mol^{-1}$).

Br_2AlN_3 attached. Obviously, the contribution of n to the thermodynamic properties matches the cluster additivity.

Thirdly, as for the isomers, their thermodynamic functions are all close at the same temperature due to that they have similar geometric and electronic structures.

Finally, based on the above discussed results, the ΔS_T, ΔH_T, and ΔG_T values in the processes of 1A $\rightarrow$ 2A, 3A, 3B, 4A, 4B, 4C, and 4D at temperatures of 200—800 K are compiled in Table 3. The ΔH_T and ΔG_T values are negative, indicating that the oligomerization is spontaneously exothermic. In addition, the ΔS_T, ΔH_T, and ΔG_T values increase from 200 K to 800 K. Thus, the binding forces of the clusters are weakened as the temperature increases.

CONCLUSIONS

In this study, we have performed a DFT study of the structure, energies, vibrational properties, and thermodynamic properties of $(Br_2AlN_3)_n$ (n = 1—4) clusters. The Al—N_α bonds form easily, and Al—Al and N_α—N_α bonds are not found in the cyclic $(Br_2AlN_3)_n$ (n = 2—4) clusters. An analysis of the geometrical parameters shows that N_2 (N_β—N_γ) and Br^- groups can be easily eliminated to yield AlN material. The energies demonstrate that the order of stability is as follows: 3A > 3B and 4B > 4C > 4A > 4D. The calculated IR spectra have three main characteristic regions: N_3 asymmetric stretching, N_3 symmetric stretching, and the complicated fingerprint region. Thermodynamic properties all increase quantitatively with increasing temperature and oligomerization degree n. Moreover, the oligomerization can occur spontaneously at temperatures up to 800 K.

This work was supported by Shandong Provincial Key Laboratory of Water and Soil Conservation & Environmental Protection (No. STKF201009).

REFERENCES

1. *Hashman T.W., Pratsinis S.E.* // J. Amer. Ceram. Soc. – 1992. – **75**. – P. 920.
2. *Lee W.Y., Lackey W.J., Agrawal P.K.* // J. Amer. Ceram. Soc. – 1991. – **74**. – P. 1821.
3. *Sheppard L.M.* // Amer. Ceram. Soc. Bull. – 1990. – **69**. – P. 1801.
4. *Saxler A., Kung P., Sun C.J. et al.* // Appl. Phys. Lett. – 1994. – **64**. – P. 339.
5. *Neumayer D.A., Ekerdt J.G.* // Chem. Mater. – 1996. – **8**. – P. 9.
6. *Boyd D.C., Haasch R.T., Mantell D.R. et al.* // Chem. Mater. – 1989. – **1**. – P. 119.
7. *Schulze R.K., Boyd D.C., Evans J.F. et al.* // J. Vac. Sci. Technol. A. – 1990. – **8**. – P. 2338.
8. *Kouvetakis J., McMurran J., Steffek C. et al.* // Main Group Met. Chem. – 2001. – **24**. – P. 77.
9. *Schulze R.K., Mantell D.R., Gladfelter W.L. et al.* // J. Vac. Sci. Technol. A. – 1988. – **6**. – P. 2162.
10. *Gladfelter W.L., Boyd D.C., Hwang J.W. et al.* // Mater. Res. Soc. Symp. Proc. – 1989. – **131**. – P. 447.
11. *Ho K.L., Jensen K.F., Hwang J.W. et al.* // J. Cryst. Growth. – 1991. – **107**. – P. 376.
12. *Dehnicke K., Strähle J., Seybold D. et al.* // J. Organomet. Chem. – 1966. – **6**. – P. 298.
13. *Müller J., Dehnicke K.* // J. Organomet. Chem. – 1968. – **12**. – P. 37.
14. *McMurran J., Kouvetakis J.* // Appl. Phys. Lett. – 1999. – **74**. – P. 883.
15. *McMurran J., Dai D., Balasubramanian K. et al.* // Inorg. Chem. – 1998. – **37**. – P. 6638.
16. *McMurran J., Kouvetakis J., Nesting D.C. et al.* // J. Amer. Chem. Soc. – 1998. – **120**. – P. 5233.
17. *Crozier P.A., Tolle J., Kouvetakis J. et al.* // Appl. Phys. Lett. – 2004. – **84**. – P. 3441.
18. *McMurran J., Todd M., Kouvetakis J.* // Appl. Phys. Lett. – 1996. – **69**. – P. 203.
19. *Dehnicke K., Krüger N.* // Z. Anorg. Allg. Chem. – 1978. – **444**. – S. 71.
20. *Xia Q.Y., Xiao H.M., Ju X.H. et al.* // J. Phys. Chem. A. – 2004. – **108**. – P. 2780.
21. *Timoshkin A.Y., Schaefer H.F.* // J. Phys. Chem. A. – 2008. – **112**. – P. 13180.
22. *Timoshkin A.Y., Schaefer H.F.* // J. Phys. Chem. A. – 2010. – **114**. – P. 516.
23. *Frisch M.J., Trucks G.W., Schlegel H.B. et al.* Gaussian 03, Revision B.03, Pittsburgh PA, 2003.
24. *Lee C., Yang W., Parr R.G.* // Phys. Rev. B. – 1988. – **37**. – P. 785.
25. *Becke A.D.* // J. Chem. Phys. – 1993. – **98**. – P. 5648.
26. *Scott A.P., Radom L.* // J. Phys. Chem. – 1996. – **100**. – P. 16502.
27. *Hill T.L.* Introduction to Statistic Thermodynamics, Addison-Wesley, New York, 1960.
28. *Xia Q.Y., Xiao H.M., Ju X.H. et al.* // Chin. J. Chem. – 2004. – **22**. – P. 1245.
29. *Xia Q.Y., Xiao H.M., Ju X.H. et al.* // Chem. J. Chin. Univ. – 2005. – **26**. – P. 922.
30. *Xia Q.Y., Xiao H.M., Ju X.H. et al.* // Int. J. Quant. Chem. – 2004. – **100**. – P. 301.
31. *Kouvetakis J., McMurran J., Steffek C. et al.* // Inorg. Chem. – 2000. – **39**. – P. 3805.